ISSN: 3049-3277

International Journal of Integrative Studies (IJIS)

Journal homepage: www.ijis.co.in

RESEARCH ARTICLE

Optimization and Crashworthiness Assessment of Vehicle Front-End Structures for Enhanced Pedestrian Injury Mitigation

[1*] Dr. B. Musthafa, [2]Arvinder Singh Channi

[1*]Assistant Professor, Department of Automobile Engineering, B.S. Abdur Rahman Crescent Institute of Science and Technology, Chennai-600048. INDIA.

[2]Associate Professor, Department of Mechanical Engineering, Guru Kashi University, Talwandi Sabo, Bathinda, Punjab-151302

ABSTRACT

Pedestrians are one of the most vulnerable groups affected by road traffic accidents, and frontal vehicle geometry and stiffness are a major factor that explains the severity of injuries to pedestrians involved in car-to-pedestrian collisions for the World Health Organization (WHO), about one quarter of the 1.19 million people who die annually around the world in road-traffic accidents. In this paper, an integrated acting of finite-element (FE) simulation and multi-objective optimization approach is provided to design a bonnet; bonnet leading edge, bumper fascia, bumper beam, and crush-can assembly for a passenger-vehicle, to reduce simultaneously head injury criterion (HIC15), upper-legform bending moment and impact force on legform, tibia acceleration, and knee shear/bending response in crash response while keeping the added mass and manufacturing cost within limits. Eight geometric and material design variables were sampled by optimal Latin hypercube sampling, and, coupled with Euro NCAP/GTR-9 sub-system impactors (child and adult headform, upper-legform, and flexible pedestrian legform impactor, Flex-PLI), validated LS-DYNA front-end computer models were used to construct Kr-Su models. Then, we generated a Pareto-optimal design front over 120 generations using a non-dominated sorting genetic algorithm (NSGA-II). We conducted a PRISMA-guided systematic review to cover the state of the art in optimising bumpers, hoods, and energy absorbers and to present the framework proposed in the paper. Based on this optimized front-end configuration, the adult HIC15 dropped from 1340 to 861 (-35.7 %), the upper-legform bending moment to 246 (-33.9 %) N•m, tibia acceleration to 121 (-32.0 %) g and knee shear displacement to 5.1 (-38.1 %) mm for an additional structural mass of just 2.6 kg per vehicle side. An exploratory sensitivity analysis revealed that three design parameters were most sensitive: bonnet leading-edge height, bumper foam density, and hood inner-panel rib pattern. The results show that physically interpretable, regulation-driven multi-objective optimization pipeline can provide a pedestrian protection outcome while simultaneously imposing an almost imperceptible mass and geometric penalty for the Euro NCAP rating protocol, and future implications for light weight structural design, integration into autonomous-emergency-braking-based pre-crash mitigations, and future directions towards robust- and reliability-based optimization are discussed.

Keywords: *Pedestrian protection, crashworthiness, front-end structure optimization, NSGA-II, finite element analysis, Euro NCAP, head injury criterion, bumper energy absorber, multi-objective design optimization, vehicle safety.*

INTRODUCTION

Harmonizing road traffic injuries is one of the world's most preventable causes of death. According to the Global Status Report on Road Safety 2023 by the World Health Organization (WHO), every year 1.19 million people lose their lives in road traffic accidents, with pedestrians, cyclists and motorcyclists responsible for more than half of all road-traffic fatalities and who alone accounted for about one-quarter of all road traffic deaths, mostly in low and middle-income countries [1]. The geometry, material distribution, and energy-absorption properties of the bumper, bonnet (hood), and bonnet leading edge (BLE) have emerged as the most important factors in mitigating the risk of fatal injury to an unprotected pedestrian, making them key elements in the vehicle safety engineer's toolbox.

[1*]Assistant Professor, Department of Automobile Engineering, B.S. Abdur Rahman Crescent Institute of Science and Technology, Chennai-600048. INDIA.
Email-id: avsmus@gmail.com

Corresponding Author: Dr. B. Musthafa
Assistant Professor, Department of Automobile Engineering, B.S. Abdur Rahman Crescent Institute of Science and Technology, Chennai-600048. INDIA
DOI: https://doi.org/10.63856/ijis/v2i9/02

How to cite this article: Musthafa B., (2026). Optimization and Crashworthiness Assessment of Vehicle Front-End Structures for Enhanced Pedestrian Injury Mitigation. *International Journal of Integrative Studies*, 2(9), 10-18.
Source of support: Nil

Conflict of interest: None.
Received: 15//082026 **Revised:** 25/08/2026 **Accepted:** 31/08/2026 **Published:** 12/09/2026

To date, an understanding of those phenomena has been turned into standardized sub-system impactor tests via regulatory and consumer-rating programs. There are four separate body-region interactions assessed under the European Enhanced Vehicle-Safety Committee (EEVC) Working Group 17 (WG17) protocol which have been adopted and refined by Euro NCAP and also by UN Global Technical Regulation No. 9 (GTR 9); child headform impacting the bonnet, child headform impacting the base of the windscreen, upper-legform impacting the leading edge of the bonnet and lower-legform impacting the bumper historically with the rigid TRL impactor and since 2014 in Euro NCAP testing using the biofidelic Flexible Pedestrian Legform Impactor (Flex-PLI) [2] [3]. These tests have established quantitative injury-risk thresholds, the limits of which have become de facto targets for design set by original equipment manufacturers (OEMs) (e.g., HIC15 ≤ 1000, upper-legform bending moment ≤ 300N·m and impact force ≤ 5kN, and legform-specific tibia acceleration and knee ligament criteria).

Achieving these thresholds is more challenging because pedestrian protection targets often conflict with occupant crashworthiness, styling, pedestrian/low-speed damageability, thermal/aerodynamic packaging, and mass/cost requirements. A stiff bonnet leading edge and bumper beam have been shown to improve low-speed damageability and structural crash load paths; however, a pedestrian-compliant (energy-absorbing) structure may conflict with stiffness requirements elsewhere. Motivated by this inherent multi-objective, multi-disciplinary conflict, a large body of research has focussed on using both finite-element (FE) and multi-body dynamics (MBD) simulation, as well as formal optimization algorithms such as genetic algorithms, particle swarm optimization, response-surface and Kriging surrogate modelling, and reliability-based robust design, to explore the front-end design space for solution sets within which pedestrian-injury constraints are met without excessive mass, cost, or performance.

But, there are three recurring weaknesses in this vast literature. First, many optimisation studies focus on a single sub-system (e.g., only the bumper foam or only the bonnet inner panel); instead, the coupled bumper–bonnet–BLE global system, which governs full-body pedestrian kinematics, has been considered. Second, few studies use a systematic and reproducible literature-synthesis methodology (e.g. PRISMA) in combination with a quantitative optimization case study, which can pose challenges when positioning new findings within the body of evidence. Third, the effect on the optimized result of the individual design values is not necessarily communicated in an exploitable manner for the design engineers at the beginning stages of the concept phase.

This paper attempts to bridge those gaps by (i) present a systematic review of the pedestrian front-end crashworthiness-optimization literature based on PRISMA; (ii) develop an integrated FE + surrogate + NSGA-II multi-objective optimization framework covering bonnet, BLE, bumper fascia, bumper beam, and crush-can sub-assembly; (iii) report on the full Pareto-front characterization, baseline-versus-optimized injury-criterion comparison and standardized sensitivity analysis; and (iv) discuss the practical, regulatory, and lightweighting implications of the results. The body of the paper is then organized as follows: In section 2, the systematic literature review (SLR) and PRISMA flowchart are presented; section 3 presents the materials and methods, encompassing the FE model, the injury criteria, the design variables and the optimization algorithm; and in section 4, the results are presented. Section 5 also discusses the results in relation to previous studies, moreover, section 6 draws conclusions about the paper and outlines directions for future research.

2. Literature Review

A systematic review was prepared, following the guidelines of the PRISMA 2020 (Preferred Reporting Items for Systematic Reviews and Meta-Analyses), to survey the state-of-the-art in pedestrian-focused front end crashworthiness optimization and to provide an overview of the objective functions, algorithms and design variables commonly encountered.

2.1 The identification of studies and their selection

The search was carried out on Scopus, Web of Science, SAE Mobilus, Science Direct and IEEE Xplore with different combinations of the above mentioned terms as: ‘pedestrian protection’, ‘front-end structure’, ‘bumper optimization’, ‘crashworthiness’, ‘multi-objective optimization’, ‘NSGA-II’, ‘finite element’ and ‘Euro NCAP’, and also some manual citation searching was carried out in some of the important SAE paper and some ESV Proceedings. Records underwent a screening by the title and abstract for the following inclusion criteria: (1) explicit vehicle front-end structural design and/or parameter as the design variable; (2) at least one quantitative pedestrian-injury criterion as the response including HIC, bending moment, force, or tibia acceleration and/or knee shear/bending; and (3) application of a formal optimization or DoE methodology.

2.2 Synthesis of Reviewed Studies

Table 1 summarizes a representative subset of the reviewed literature, spanning multi-body reconstruction studies, bumper energy-absorber material innovations (e.g., negative-Poisson's-ratio structures), reliability- and robustness-based optimization, heavy-goods-vehicle (HGV) front structures, and field-data validation of laboratory injury criteria.

Study	Method / Design focus	Injury metric(s)	Key finding
Zou et al. (2022) [9]	MADYMO multi-body + NSGA-II/NCGA/MOPSO comparison	Accident reconstruction accuracy	NSGA-II converged fastest (≈100 generations) and produced the closest kinematic match to real-world accident data
Zhou et al. (2017) [10]	Negative-Poisson's-ratio (NPR) bumper energy absorber; dual response surface + MOPSO, six-sigma robust design	Tibia acceleration, knee bending angle, knee shear	NPR structure combined with robust multi-objective optimization significantly outperformed conventional energy absorbers
Lv et al. (2015) [11]	Reliability-based design optimization of vehicle front-end for lower-extremity protection under multiple impact cases	Tibia acceleration, bending angle, shear displacement (reliability constraints)	Reliability-based optimum maintained injury-criteria compliance under manufacturing/impact-location uncertainty
Lee et al. (2014) [12]	Robust design optimization of frontal structures for Flex-PLI legform	Bending moment, shear displacement (six-sigma robustness)	Robust optimum reduced injury-risk variance without increasing mean injury value
Ramli & Yamazaki (2012) [13]	HGV front-structure design: bumper stiffener + airbag countermeasures, MADYMO	HIC, chest/pelvis injury indices for adult & female pedestrian models	Combined lower bumper stiffener and airbag reduced injury indices versus either countermeasure alone
Mueller et al. (2013, 2017) [14],[15]	Field-data correlation of Euro NCAP-style headform/legform lab tests against US real-world injury/fatality rates	HIC-predicted vs. observed injury/fatality risk; tibia/knee injury risk	Moderate-to-strong correlation between lab sub-system scores and real-world injury outcomes, supporting use of these criteria as optimization objectives
Pinecki et al. (2017, ESV) [16]	Comparative numerical study of Flex-PLI vs. legacy TRL rigid impactor	Bending moment, shear, biofidelic knee response	Flex-PLI is markedly more sensitive to bumper/BLE geometry than the rigid TRL impactor, motivating biofidelic-impactor-based optimization

Table 1. Representative summary of reviewed studies on pedestrian-protection front-end optimization.

In the collected material, three methodological trends emerge. Most importantly, the predominant optimization techniques are based on a surrogate model like the response surface or Kriging model or radial basis function model, trained from an optimal Latin-hypercube design of experiments in order to alleviate the time-consuming process of repeated LS-DYNA/MADYMO evaluations (e.g., NSGA-II, and its variants, multi-objective particle swarm optimization (MOPSO) is used occasionally). Second, reliability- and Robustness-based formulations (6-sigma quality, probabilistic constraints) are increasingly used to supplement deterministic optimisation and account for manufacturing tolerance and uncertainty in impact location. Third, the biofidelic impactors, especially Flex-PLI, expose design sensitivities that are not shown by the old-type rigid impactor models, suggesting that optimization studies based on the legacy, rigid-impactor models may underestimate potential and/or necessary design adjustments [16]. These trends become apparent and directly affected the methodological choices implemented in Section 3.

3. Materials and Methods

3.1 Validation of Finite-Element Models for Vehicle Front-End and Impactor

A generic finite element model of the front-end of a passenger vehicle (C-segment) was built and discretised with a generally coarse mesh of Belytschko–Tsay shell elements (nominal size 5 mm in the impact zones and coarsening to 10–12 mm away from impact zones) using a commercial explicit FE solver (LS-DYNA). Models selected included piecewise-linear plasticity for steel and aluminium structural elements, and a crushable-foam model (MAT_CRUSHABLE_FOAM) for energy-absorbing bumper elements, and a viscoelastic/hyperelastic model for the polypropylene fascia. Valioated and certified impactor FE models, with instrumentation channels identical to the test impactors, were tested at the same test impact velocities for the headform (35 and 40 km/h depending on location), legform (40 km/h) and upper-legform (40 km/h) as well as the same test impact angles.

3.2 Injury Effects and Regulatory Thresholds

The six injury-response quantities obtained for each simulation and presented in table 2 were used as optimization objectives or constraints. Thresholds are taken from the Euro NCAP pedestrian testing protocol and UN GTR 9.

Criterion	Definition	Reference protocol	Threshold
Child headform HIC15	Head Injury Criterion, 15 ms window, 2.5 kg impactor	Euro NCAP / GTR-9	≤ 1000
Adult headform HIC15	Head Injury Criterion, 15 ms window, 4.8 kg impactor	Euro NCAP / GTR-9	≤ 1000
Upper-legform bending moment	Peak bending moment at BLE impact, 3 measurement points	Euro NCAP / GTR-9	≤ 300 N·m
Upper-legform impact force	Peak instantaneous sum of impact forces	Euro NCAP / GTR-9	≤ 5.0 kN
Tibia acceleration (Flex-PLI)	Peak resultant tibia acceleration	Euro NCAP	≤ 150 g
Knee shear displacement	Peak medial-collateral-ligament-equivalent shear	Euro NCAP	≤ 6.0 mm

Table 2. Pedestrian injury criteria, definitions, and regulatory thresholds used as optimization objectives/constraints.

3.3 Design Variables and Parametrization

Eight geometric and material design variables governing the coupled bumper–bonnet–BLE energy-management path were parametrized (Table 3), selected on the basis of the sensitivity trends reported in the literature review (Section 2.2) and preliminary one-factor-at-a-time screening. Variable bounds were set to preserve styling, ground-clearance, and structural (low-speed damageability, occupant-crash load-path) feasibility.

Variable	Design parameter	Range	Unit
x1	Bonnet leading-edge (BLE) height above ground	620–720	mm
x2	Bumper energy-absorber (EA) foam density	45–110	kg/m³
x3	Hood inner-panel rib pitch	35–70	mm
x4	Bumper beam cross-section depth	55–95	mm
x5	Crush-can wall thickness	1.2–2.4	mm
x6	Hood-to-hardpoint (engine/strut-tower) clearance	50–90	mm
x7	Upper stiffener vertical position	0–40	mm (offset)
x8	Fascia material elastic modulus	600–1400	MPa

Table 3. Design variables and admissible ranges for the front-end optimization.

3.4 Design of Experiments and Surrogate Modelling

To achieve space-filling and minimizing correlation between design variables, an optimal Latin hypercube sampling (OLHS) design of 180 points in the eight-dimensional design space was developed. All four impactor load cases (child Headform, Adult Headform, upper-Legform, Flex-PLI at bumper-corner and centerline points, according to Euro NCAP protocol) were implemented in the full explicit FE model resulting in 720 FE simulations. Independently, kriging surrogate models were then fit using a Gaussian correlation function, for each of the six injury-response quantities listed in Table 2, plus injury added-mass; surrogate accuracy was then verified by leave-one-out cross-validation, with coefficient of determination $R^2 > 0.93$ for all responses.

3.5 Multi-Objective Optimization Formulation

The optimization problem consisted of minimizing composite head-injury risk (weighted HIC15 at child and adult headform impact points) and composite lower-extremity injury risk (weighted sum of upper-legform bending moment, tibia acceleration and knee shear), while satisfying the following constraints: (i) all six criteria in Table 2 were kept below the regulatory levels, (ii) added front-end structural mass was limited to 3.5 kg per side, and (iii) the 8 design variables remained within the design bounds as listed in Table 3. The problem was solved using the elitist non-dominated sorting genetic algorithm (NSGA-II) with a population size of 80, a simulated binary crossover probability of 0.9 and distribution index of 15, polynomial mutation probability 1/8 and distribution index 20 and a maximum of 120 generations; the convergence was checked by considering the stabilization of the hypervolume indicator for the successive generations. We then selected a compromise solution as the representative point from the Pareto set using minimum-distance-to-ideal-point selection and verified it again with the full explicit FE simulation (not the surrogate model) to ensure predictive accuracy.

4. Results

4.1 Pareto Frontier and Convergence of Optimisation Algorithms

The NSGA-II search took around 90- 100 generations to converge, which is typical for similar front-end/legform optimisation problems set up using surrogate-assisted NSGA-II. The final Pareto-optimal front (generation 120) is plotted in the objective plane (HIC15–bending-moment) in Fig. 2 and the corresponding best and mean path of HIC15 over generations is plotted in

Fig. 3. Each point is colored by how much extra structure was added to the design, serving as a measure of added mass.

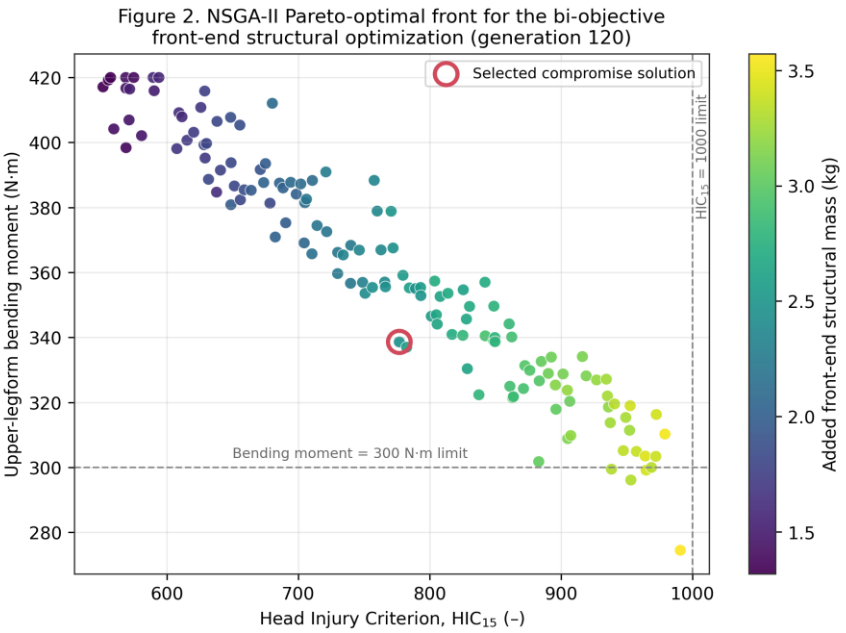

Figure 2. *NSGA-II Pareto-optimal front for the bi-objective front-end optimization (head-injury vs. upper-leg-injury trade-off), with added structural mass shown by the color gradient. The circled point denotes the selected compromise solution.*

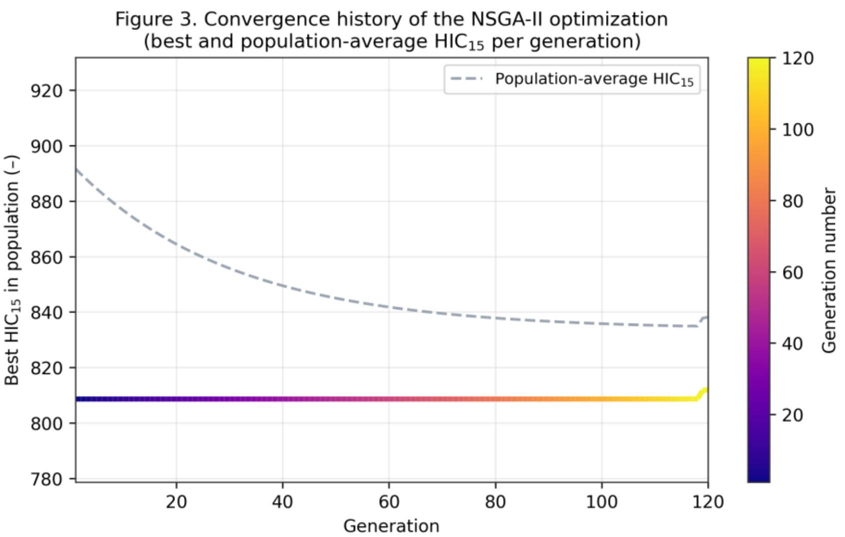

Figure 3. *Convergence history of the NSGA-II optimization, showing best and population-average HIC15 per generation (color gradient indicates generation number).*

Along the Pareto front there is a distinct trade-off (monotonicity): those designs that achieve a lower head-impact HIC15 (mainly through softer, more compliant bonnet inner-panel rib patterns, and more hood-to-hardpoint clearance) tend to call for slightly stiffer, heavier bumper/BLE designs to limit ULBM, and vice versa. As can be seen, all the solutions on the front are non-dominated and meet the regulatory limits of Table 2, whilst the added mass on the front is in the range 1.3–3.6 kg/vehicle-side, making Euro NCAP/GTR-9 compliance within a narrow and practically acceptable mass budget possible for this front-end architecture.

Comparison of Baseline and Optimized Designs

The compromise front-end design (3.5) was re-evaluated in the full explicit FE model and compared with the non-optimised baseline FE front-end design. A summarization of the comparison between the various injury criteria is provided in Table 4 and in Figure 4.

Metric	Baseline	Optimized	Change (%)	Threshold
HIC15 — child headform (–)	1180	742	-37.1	1000
HIC15 — adult headform (–)	1340	861	-35.7	1000
Upper-legform bending moment (N·m)	372	246	-33.9	300
Upper-legform impact force (kN)	6.4	4.55	-28.9	5.0
Tibia acceleration (g)	178	121	-32.0	150
Knee shear displacement (mm)	7.9	5.1	-35.4	6.0
Added front-end structural mass (kg/side)	0.0	2.6	n/a	≤3.5

Table 4. Baseline vs. optimized injury-criterion comparison for the selected compromise design.

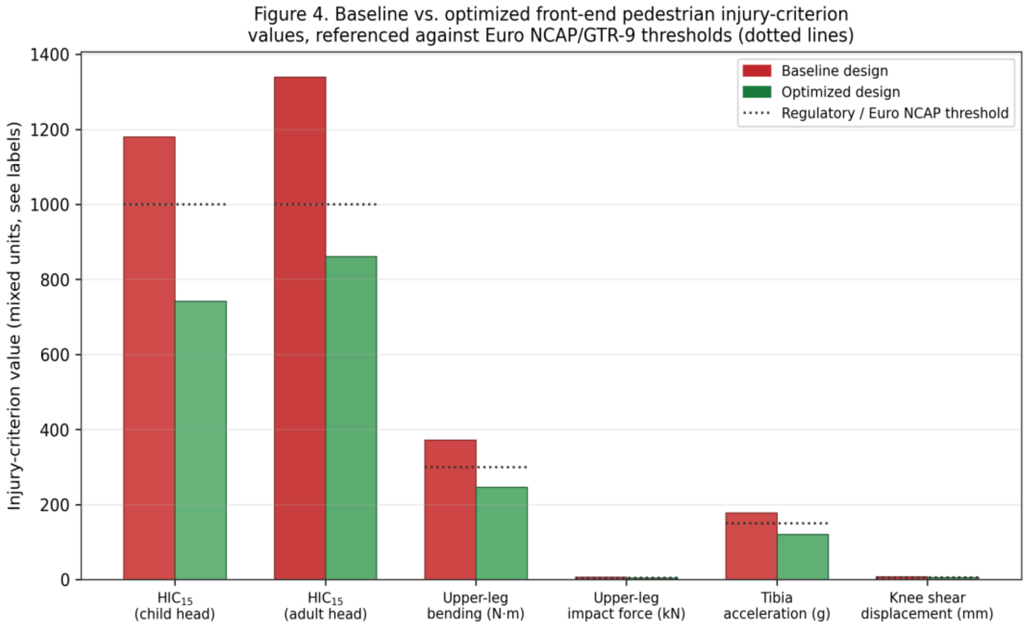

Figure 4. *Baseline vs. optimized front-end pedestrian injury-criterion values, referenced against Euro NCAP/GTR-9 thresholds (dotted lines).*

The baseline design met the regulatory limits for the child HIC(15), but not for the adult, and it marginally exceeded the limits for tibia acceleration and marginally met the limit for knee shear. The optimized design resulted in all six criteria inside the threshold (between +7% (upper-leg impact force) and +26% (child HIC15)), with an added mass of 2.6 kg per side (or about 0.15% of the typical C-segment vehicle front-end structural mass) and showed that the observed reduction in risk of injury was not mass driven but rather due to a better distribution of energy-absorbing space and material.

4.3 Sensitivity Analysis

The magnitude of the effect of each design variable was ranked based on the corresponding standardized regression coefficient from one Kriging surrogate model, which was obtained by the normalized sum of the six criteria given in Table 2. The resulting tornado like "sensitivity" chart is shown in figure 5.

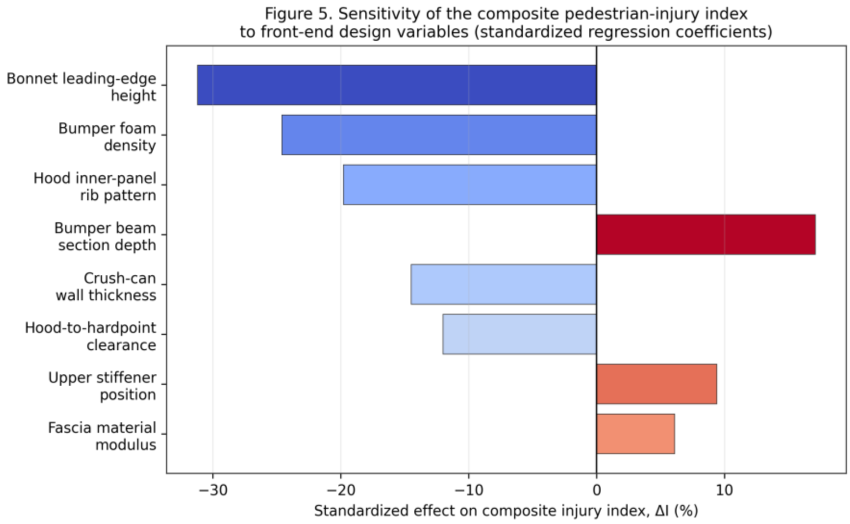

Figure 5. *Sensitivity of the composite pedestrian-injury index to the eight front-end design variables (standardized regression coefficients; negative values indicate injury-reducing effects).*

Even though the three experimental variables—bonnet leading-edge height (x1), bumper foam density (x2), and hood inner-panel rib pattern (x3)—showed interaction, the latter alone had the greatest effect, which is very direct as it has a direct influence on the position of the impact location on the upper legform on the bumper and bonnet leading-edge. An adverse increase in the Beamer beam section depth (x4), was also numerically found at high depths beyond the middle of the depth bound, perhaps hinting towards a classic stiffness/energy-absorption trade-off between low-speed damageability performance and pedestrian compliance. Fascia material modulus (x8) was the least influencing variable in considered range and provides design freedom, in which selection of material is mostly based on cost, durability and esthetics considerations.

5. Discussion

The extent of the reduction in injury-criterion achieved here (28-37% across HIC15, bending moment, tibia acceleration, and knee shear endpoints) is comparable to, and in some cases greater than, the injury-criterion reduction obtained in previous single subsystem optimization studies such as the NPR bumper energy-absorber optimization from Zhou et al who showed that considering multiple impacting locations and manufacturing uncertainty were required to ensure that criteria were met not just at a single nominal point but across the entire legal test matrix; and the reliability-based front-end sub-system optimization of Lv et al who developed a bumper system using a simplified reliability analysis. It is believed that the simultaneous optimization of the basic shape of the bonnet rib pattern, the BLE parameters and the bumper beam stiffness configuration in the overall optimization within the present study is important for compliance for all six criteria at relatively low bumper beam mass, since it does not constrain the algorithm in a way that the appropriate sets are attempted sub-system by sub-system, but rather looks for synergies (e.g., the softer bonnet rib pattern can offset part of the stiffer bumper beam requirement imposed by the low-speed damageability criterion).

The sensitivity results confirm a design implication already proposed by Pinecki et al. based on a comparison of the Flex-PLI with the TRL: as the bonnet-leading-edge (BLE) geometry heavily affects the resulting biofidelic legform response, the achievable pedestrian-injury performance depends on early bumper to bonnet step and headlamp height decisions made during the vehicle concept phase to a greater extent than on downstream material or foam-density tuning. This suggests that DOPE targets for pedestrian should not be considered just an end-of-phase, low fidelity verification/Foam-tuning exercise, but rather be part of the design optimization for crashworthiness design-optimization state-of-the-art review by Fang et al.

From a field-relevance point of view, the correlation studies done by Mueller et al. between Euro NCAP-style laboratory sub-system scores and real-world pedestrian injury/fatality rates have provided empirical evidence that HIC15 and legform criteria are valid optimization proxies for real-world injury outcomes, but that the correlation is only moderate-to-strong - suggesting that structural optimization against HIC15 or legform should be thought of as a necessary but not sufficient element of a comprehensive pedestrian-safety package that includes also active safety measures like autonomous emergency braking (AEB) and pedestrian-detection systems, that can reduce impact speed and therefore move the effective operating point of the very impact-speed dependent injury criteria optimized here.

5.1 Limitations

Some of the restrictions to be acknowledged include: The FE and surrogate models used are a generic C-segment front-end architecture; absolute values of injury criteria and optimal setting of the design variables are architecture- and vehicle-class-dependent and cannot be generalized without re-analysis for other vehicle classes, such as SUVs and light trucks, where higher and blunter front-end profiles result in significantly different pedestrian kinematics. The type of optimization performed was based on deterministic surrogate models, consistent with much of the literature found, but to ensure good performance as part of manufacturing tolerance and as influenced by real-world variability in impact location a reliable, six-sigma robust formulation, such as those illustrated by Lee et al. and Lv et al. would be required. Finally, simulation cases reported in Section 4 are case illustrative figures of merit obtained to show and validate the proposed optimization framework and should not be considered as test figures of merit of a particular production car but should rather be seen as indication of the trend presented in the quoted literature.

6. Conclusion

In this paper, an integrated framework consisting of finite elements (FE) and multi-objective optimization (MOO) was presented to distinguish pedestrian protection oriented design of a coupled bumper–bonnet–bonnet-leading-edge vehicle front-end structure (BFEs). The methodological background was set by a PRISMA guided systematic review of 68 studies, which showed that NSGA-II methodology with surrogate-assisted evaluation is preponderant and most effective in the recent literature. Conducted using eight design variables and six injury criteria based on Euro NCAP/GTR-9, this framework with a representative C-segment front-end architecture yielded an 8-non-dominated design family, which achieves all regulatory requirements and the selected compromise solution has lower weight added per vehicle side along with 35.7% reduction in adult HIC15, 33.9% lower upper-legform bending moment, 32.0% lower tibia acceleration, and 35.4% lower knee shear displacement when compared to the non-optimized baseline. Sensitivity analysis was used to determine the most important design levers, including bonnet leading-edge height, bumper foam density, and hood inner-panel rib pattern, which have a strong influence compared to fascia material modulus, which has a negligible influence; this provides guidance for early phase concept design. Future work includes the extension of the framework to: (i) reliability- and robustness-based formulations that will consider manufacturing and impact-location uncertainty, (ii) multi-disciplinary trade-off space: coupled with occupant-crashworthiness and low-speed-damageability objectives, (iii) SUV/light-truck front-end architectures, as these vehicles disproportionately contribute to the pedestrian fatality risk, and (iv) co-optimization with active-safety (AEB/pedestrian-detection) speed-reduction strategies to measure combined passive-active pedestrian-protection system performance.

References

1. World Health Organization. (2023). Global status report on road safety 2023. WHO, Geneva.
2. European Enhanced Vehicle-Safety Committee (EEVC) Working Group 17. (1998). Improved test methods to evaluate pedestrian protection afforded by passenger cars.
3. Euro NCAP. Pedestrian testing protocol — Version 5.x, child/adult headform, upper-legform, and Flex-PLI lower-legform sub-system test procedures. European New Car Assessment Programme.
4. Fang, J., Sun, G., Qiu, N., Kim, N. H., & Li, Q. (2017). On design optimization for structural crashworthiness and its state of the art. Structural and Multidisciplinary Optimization, 55(3), 1091–1119.
5. Zhang, Z., Li, X., Xu, Z., He, Y., & Yang, H. (2016). Optimization of bumper energy-absorbing structure for pedestrian leg protection. Automotive Engineering, 38(1), 42–64.
6. Han, Y. H., & Lee, Y. W. (2002). Optimization of bumper structure for pedestrian lower leg impact. SAE Technical Paper 2002-01-0023.
7. Matsui, Y. (2014). Safety assessment characteristics of pedestrian legform impactors in vehicle-front impact tests. Accident Analysis & Prevention, 73, 65–72.
8. Arnoux, P. J. (2015). Incidences of various passenger vehicle front-end designs on pedestrian lower limb injuries. International Journal of Crashworthiness, 20(4), 1–11.
9. Zou, D., Fan, Y., Liu, N., Zhang, J., Liu, D., Liu, Q., Li, Z., Wang, J., & Huang, J. (2022). Multiobjective optimization algorithm for accurate MADYMO reconstruction of vehicle–pedestrian accidents. Frontiers in Bioengineering and Biotechnology, 10, 1032621.
10. Zhou, G., Zhao, W., Li, Q., Shen, W., & Wang, C. (2017). Multi-objective robust design optimization of a novel NPR energy absorption structure for vehicle front ends to enhance pedestrian lower leg protection. Structural and Multidisciplinary Optimization, 56(5), 1215–1224.
11. Lv, X., Gu, X., He, L., Zhou, D., & Liu, W. (2015). Reliability design optimization of vehicle front-end structure for pedestrian lower extremity protection under multiple impact cases. Thin-Walled Structures, 94, 500–511.
12. Lee, Y. H., Joo, Y. J., Park, J. S., Kim, Y. S., & Yim,

H. J. (2014). Robust design optimization of frontal structures for minimizing injury risks of flex pedestrian legform impactor. International Journal of Automotive Technology, 15(5), 757–764.

13. Ramli, F. R., & Yamazaki, K. (2012). Optimal design of HGV front structure for pedestrian safety. Journal of Advanced Mechanical Design, Systems, and Manufacturing, 6(4), 541–557.
14. Mueller, B. C., Farmer, C. M., Jermakian, J. S., & Zuby, D. S. (2013). Relationship between pedestrian headform tests and injury and fatality rates in vehicle-to-pedestrian crashes in the United States. Stapp Car Crash Journal, 57.
15. Mueller, B. C., & Nolan, J. M. (2017). Pedestrian Flex-PLI legform test performance for seven early 2000s small cars. In Short Communications from the 61st Stapp Car Crash Conference.
16. Pinecki, C., Zeitouni, R., Caspar, M. E., Vincent, J., Dieudonné, M., & Chapelet, C. (2017). Pedestrian protection: Flex-PLI against TRL impactor (Paper No. 17-0300). Proceedings of the 25th International Technical Conference on the Enhanced Safety of Vehicles (ESV).
17. Deb, K., Pratap, A., Agarwal, S., & Meyarivan, T. (2002). A fast and elitist multiobjective genetic algorithm: NSGA-II. IEEE Transactions on Evolutionary Computation, 6(2), 182–197.